FAST RANDOM WALKER FOR NEUTROPHIL CELL SEGMENTATION IN 3D

Cheng-Jin Du, John G. Ferguson†, Phillip T. Hawkins†, Len R. Stephens†, Till Bretschneider**
*Warwick Systems Biology Centre, University of Warwick, Coventry, CV4 7AL, UK; †The Babraham Institute, Cambridge, CB22 3AT, UK.

ABSTRACT

The random walker method [1] has many nice characteristics for 3D image segmentation. However, it is computational expensive and slow due to a massive linear system to be solved. In this work, we take advantage of the probabilistic output from the random walker method applied to a small downsampled image. By using the original image and seeds information, a novel edge-preserving method is introduced to upsample the probability, which is used for final segmentation. The running time is significantly reduced, taking less than one second to segment a 180×283×12 image stack on a normal laptop. Furthermore, the proposed method performs better when dealing with noisy boundaries than the original random walker method and the level set method.

Index Terms— Random walker, neutrophil cell segmentation, 3D cell segmentation, edge-preserved upsampling, cell motility

1. INTRODUCTION

Our current view of moving neutrophil cells is mostly based on 2D cross-sections through the cell centre or TIRFM studies of the substrate attached cell surface. To better understand cellular mechanics and obtain an integrated view of cell motion, a full 3D analysis is required, including 3D segmentation, surface reconstruction, and local measurements of membrane deformations. Spinning disk confocal microscopy allows us to acquire time series of 3D stacks within seconds, but because of short exposure times signal-to-noise ratios are low. Further complications are inhomogeneous labeling (e.g. the intensity of the cell interior similar to that of the background in Fig. 1(b)), and ambiguous boundaries, making segmentation non-trivial.

A variety of algorithms for cell segmentation have been proposed in the literature, mainly in 2D. A popular technique is the region-growing method [2], which works well for homogeneous and separated cells. However, it suffers from over-segmentation when intensities vary spatially inside cells. Other methods are seeded watershed algorithms [3], active contours [4], graphical models [5], active mask [6], and graph Laplacian diffusion based methods [7]. Most approaches are semi-automatic due to the complexity of cell images, requiring users to draw scribbles as seeds or a window around the cell to be segmented.

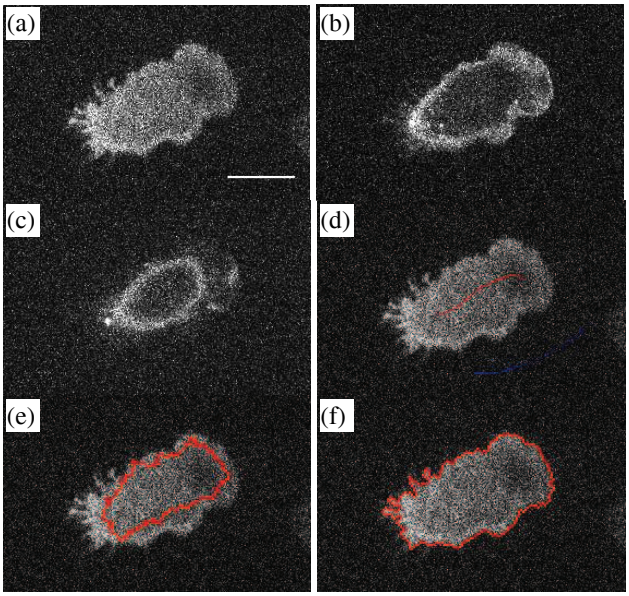


Fig. 1. A 3D stack (12 slices) of a neutrophil cell labeled with cell mask orange dye. (a-c) are the 1st, 4th, and 7th slices. (d) The first slice with scribbles as seeds for segmentation. (e) Segmentation obtained by the random walker method [1]. (f) Segmentation using our method. Scale bar: 10 micron.

Graph based methods have achieved impressive results by constructing a graph where nodes correspond to image pixels and edges connect nearby pixels with weights reflecting similarities in image intensity. In this paper, we use a random walker approach for cell segmentation [1], which has many nice characteristics, including trivial generalization to simultaneous multi-region and 3D segmentation, robustness to noise, weak boundaries detection, a sound theoretical basis, and a probabilistic output that can be employed to identify areas of uncertainty. However, since a massive linear system needs to be solved when segmenting a 3D image stack, computational costs are high. Other downsides are limited abilities to segment noisy boundaries as shown in Fig. 1(e), which uses the seeds of Fig. 1(d) and the code from the author's website for 2D segmentation. Additionally, when extended to 3D segmentation of the stack of Fig. 1(a-c), the random walker method of [1] failed to produce reasonable results as shown in Fig. 3.

By taking advantage of the time that images are stored on servers prior to an analysis, offline precomputation was proposed to speed up this popular algorithm [8,12]. However, that is not an ideal solution. Besides the extra offline precomputation time, large storage space is required for precomputed matrices. In this paper, we downsample images with a rate of 1/8 or less to obtain initial results by making use of the probability outputs from the random walker method. Our key contribution is to introduce a novel quick edge-preserved method to upsample the probability for segmentation by using the prior original image and seeds information. Computational time is significantly reduced, which takes less than one second to segment a 180×283×12 image on a normal laptop. Furthermore, the proposed method deals better with the noisy boundaries as shown in Fig. 1(f) that is segmented in 2D using our method (for the reason of comparison with Fig. 1(e)).

2. FAST RANDOM WALKER

We begin by briefly explaining notations. Given an image with N pixels, a weighted undirected graph $G = (V, E, A)$ with vertices $v \in V$ and edges $e \in E$ is constructed. Each pixel corresponds to a vertex v, and each pair of neighboring vertices is connected by an edge e. The connectivity will be 4 or 8 for 2D images, and 6 or 26 for 3D ones. $A \in R^{N \times N}$ is a weighted affinity matrix, which maps changes in the image structure to edge weights. Let D be a diagonal matrix with elements given by degrees of vertices $d_i = \sum_{j \in V} A_{ij}$. The weighting function is defined as

$$A(i, j) = \exp(-\left\|S_i - S_j\right\|^2 / \sigma_S - \left\|I_i - I_j\right\|^2 / \sigma_I) \qquad (1)$$

where I_i is the image intensity value at vertex v_i, and S_i indicates its spatial position. The graph Laplacian matrix is then given by $L = D - A$.

2.1. Random walker method

The random walker method proposed in [1] finds the probabilities of unseeded nodes by

$$\min \; x^T L x = \sum_{e_{ij} \in E} w_{ij} (x_i - x_j)^2 \qquad (2)$$

Based on the provided seeds, Eq. (2) can be decomposed into

$$\min \quad [x_M^T \; x_U^T] \begin{bmatrix} L_M & B \\ B^T & L_U \end{bmatrix} \begin{bmatrix} x_M \\ x_U \end{bmatrix} \qquad (3)$$

where x_M and x_U correspond to the probabilities of seeded and unseeded nodes respectively. The optimization problem of Eq. (3) can be solved by the linear equation:

$$L_U x_U = -B^T x_M \qquad (4)$$

This is a large linear system for 3D segmentation of a cell image. Although Eq. (4) is a sparse, symmetric and diagonally dominant system, solving it directly will be still slow requiring $O(U)$ running time.

2.2. Downsampling

Obviously, if we reduce the number of unseeded nodes, the time for solving Eq. (4) can be reduced. The problem is how to reduce the number of equations without sacrificing the accuracy of the algorithm. We first downsample the image using the bilinear method to make it substantially smaller. Since the resolution in z is much lower than in x and y, we do not downsample in z. The random walker method is then applied to the downsampled stack, with much fewer equations to be solved.

2.3. Seeds propagation

Segmentation begins with the user roughly scribbling parts of the image that belong to either cell or background. We mark the seeds in the original image, and scale their positions in the downsampled image for the initial segmentation. Caution should be taken to remove duplicated seeds, which end up in the same position. This should not affect the final segmentation result. When scribbles are placed inside an object, the scaled down seed locations should still lie within the downsampled object.

Compared with 2D images, it will require considerably more user effort to seed a noisy 3D image with many slices. We propose to use only the bottom slice of the cell volume for seeding in 2D. The seeds are then propagated to the entire volume by a simple thresholding method. The threshold value is calculated as

$$T = \mu_{seeds} + \sigma_{seeds} \qquad (5)$$

where μ_{seeds} and σ_{seeds} are the intensity mean and standard deviation of seeded pixels of the cell in the bottom slice. We only generate extra seeds for the cell, not for the background. As shown in Fig. 1(b-c), the cell interior has similar intensity values as the background. However, we are confident that high intensity pixels belong to the cell.

In [9], Grady introduced regional intensity priors into the formulation of Eq. (2) to segment disjoint regions, as the segmentation of Eq. (4) is based on localized image data only and disconnected regions must be seeded individually. The prior probability λ is derived from the seeded pixels using a Gaussian kernel. The original random walker problem solved on the augmented Laplacian becomes [8]

$$(L_U + \gamma I_U) x_U = \gamma \lambda - B^T x_M \qquad (6)$$

where γ is a parameter to weight the prior probability, and I_U is an identity matrix.

Our method to propagate seeds is also based on density estimation derived from seeded pixels. However, our method is simpler and much faster. Furthermore, the prior computation method of [9] is actually not so suitable for our application due to the similar intensities of background and

cell interior. For other applications such as the images in [8] where the intensity is different from background, our framework can be employed to speed up the solution of Eq. (6) as well.

2.4. Edge-preserved upsampling

The random walker method (Section 2.1) is applied to the downsampled image (Section 2.2) with propagated seeds (Section 2.3). The obtained downsampled probability is extrapolated by a cubic method to the original image size. The upsampled probability q_i^c at pixel i is calculated in the following form:

$$q_i^c = \frac{1}{|neighb(i)|+1} \sum_{k\in\{neighb(i),i\}} w(I_i, \mu_{seed}^c)(p_i^c + \eta) \qquad (7)$$

where c is the class indication of cell or background, I_i is the intensity at pixel i of the original image, p_i^c is the extrapolated probability of class c at pixel i, and η is a parameter to balance the importance of the weight $w(I_i, \mu_{seed}^c)$ given by

$$w(I_i, \mu_{seed}^c) = \begin{cases} (1-((I_i-\mu_{seed}^c)/\tau)^2)^2 & |I_i-\mu_{seed}^c| \le \tau \\ 0 & otherwise \end{cases} \qquad (8)$$

where τ is a scale parameter in the intensity domain. Eq. (8) gives higher weight to pixels with intensities similar to the mean intensity of seeds. If the intensity difference is bigger than τ, the weight is set to zero. The final segmentation is obtained by assigning the pixel i to the class corresponding to $\max_c(p_i^c)$.

The effect of Eq. (8) is similar to Tukey's biweight edge-stopping function introduced in [10] for robust anisotropic diffusion. The discrete diffusion equation governing the value I_i^{t+1} is

$$I_i^{t+1} = I_i^t + \frac{\alpha}{|neighb(i)|} \sum_{k\in neighb(i)} g(I_k^t - I_i^t)(I_k^t - I_i^t) \qquad (9)$$

where t is the time step, α determines the rate of diffusion, and $g(\cdot)$ is an edge-stopping function. The choice of $g(\cdot)$ can greatly affect the extent to which discontinuities are preserved. A variety of edge-stopping functions have been used such as Lorentz, Gauss, and Tukey's biweight function [10], which are plotted in Fig. 2. It is helpful to understand how an edge-stopping function deals with outliers. We can see that the Lorentz function gives more influence to outliers than the Gauss and the Tukey functions. More robust results can be achieved by Tukey's biweight function, as it completely prevents diffusion across edges.

In [10], the intensity difference is calculated between the pixel i and its neighboring pixels as seen in Eq. (9). For regions of piecewise constant intensity, anisotropic diffusion is equivalent to average intensities of neighbor pixels. For an

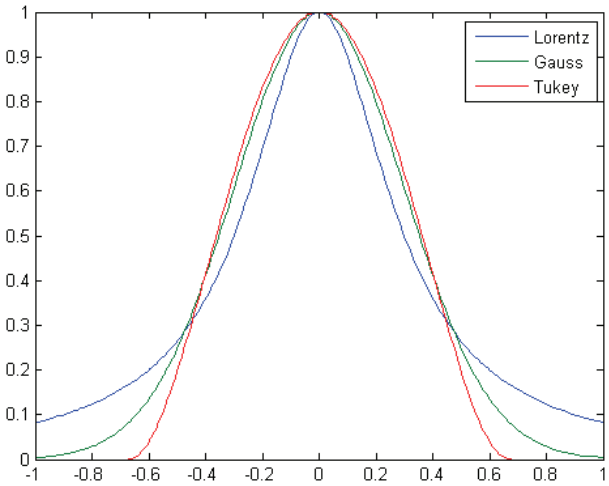


Fig. 2. Comparison of edge-stopping functions.

image region that includes boundaries, the influence of "outliers" is low as the value of $g(\cdot)$ is small for large intensity differences. However, our method computes intensity differences between the pixel i and the mean of seeded pixels, instead of its neighboring pixels. To make it more clear, Eq. (7) can be rewritten as

$$q_i^c = \frac{1}{(|neighb(i)|+1)|seed^c|} \sum_{k\in\{neighb(i),i\}} \sum_{j\in seed^c} w(I_i, I_j^c)(p_i^c + \eta)$$

Here, the edge-stopping property is nicely kept, and "outliers" can be explained explicitly as pixels belonging to a class other than c.

The final segmentation result will contain some small spurious objects due to few high intensity pixels in the background. The morphological close operator was used to remove those falsely detected small objects.

3. RESULTS

The experiments were performed using unoptimized Matlab code running on an Intel(R) Core(TM) 2.3GHz with 6GB of RAM. Ten stacks of neutrophil images were tested, labeled with cell mask orange dye to stain the plasma membrane. The neutrophils are sitting quiescent, then are stimulated by application of fMLP which prompts cell spreading and movement. Cell movements are imaged by spinning disk confocal microscopy. We use raw data to test our method, which are more challenging than deconvolved data. Although the deconvolution usually generates smoother data, it is prone to generate artifacts.

We compared both the segmentation quality and the time complexity of our method with the random walker [1] and the level set method [11]. For the random walker method, we propagated the seeds similarly as described in Section 2.3 using the original image. We extended the code from [1] to 3D image segmentation. For the level set method, we manually set a region of interest with a right

prism and then run the algorithm with 50 iterations using the code from [11]. We use the subsampling rate of 1/8 for all the test image stacks.

Fig. 3 shows the results for the segmentation of the stack shown in Fig. 1. The random walker method was unable to obtain a proper result, possibly because of the noise in the image and the inhomogeneous intensity distribution. We also tried to use the bilateral filter to denoise the slices first before segmentation, but still without much improvement. Our method is comparable to the level set method with respect to dealing with noisy cell boundaries, but produces a cleaner output. Regarding efficiency, our method took only 0.95s, while the random walker method and the level set method took 12.3s and 32.09s, respectively. Fig. 4 shows the segmentation results of three other stacks using our method. It can be seen that currently our method struggles to segment very fine cell processes (retraction fibers), which deserve further study.

The global F-measure [13] is calculated to evaluate the segmentation results quantitatively. The ground truth of the whole cell was obtained manually. As the random walker method cannot segment the cell with enclosed boundary, we only compare our approach with the level set method. Our method achieves better F-measure value of 0.89, when compared with the level set method of 0.83.

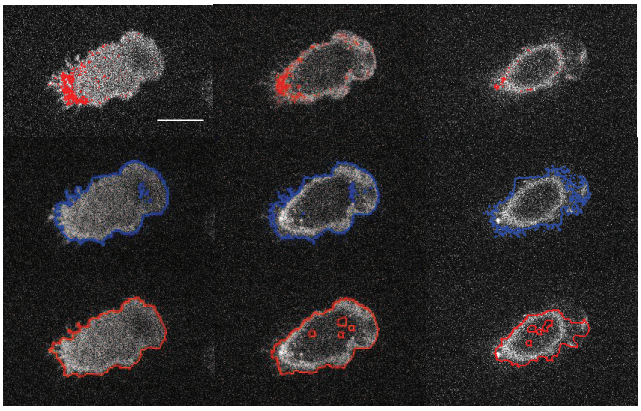


Fig. 3. Comparison of segmentation results by using the random walker method (Row 1), the level set method (Row 2), and our method (Row 3). Scale bar: 10 micron.

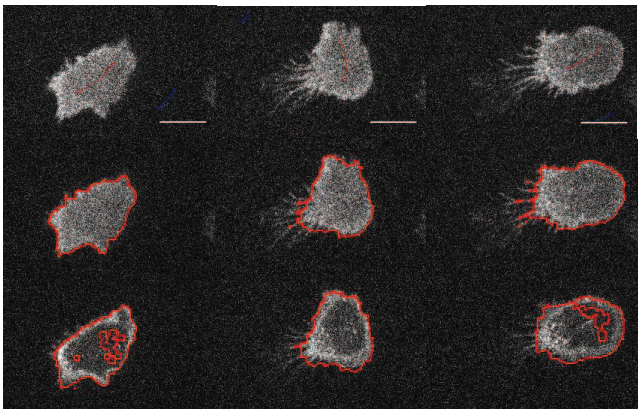


Fig. 4. Scribbles and segmentation results using our method for three other stacks. Scale bar: 10 micron.

4. CONCLUSIONS

The method we propose is faster than the random walker method and the level set method, while segmentation performance is better for noisy 3D neutrophil cells. It naturally inherits the characteristics of the random walker method but deals better with noisy boundaries. The techniques can be used to speed up other segmentation methods such as the random walker with priors [9].

5. REFERENCES

[1] L. Grady. “Random walks for image segmentation,” *IEEE TPAMI*, 28(11), 1768–1783, 2006.

[2] T.R. Jones, A. Carpenter, and P. Golland, "Voronoi-based segmentation of cells on image manifolds," *In Proceedings of CVBIA'2005*, vol. 3765, pp. 535-543, 2005.

[3] G. Lin, M.K. Chawla, K. Olson, C.A. Barnes, J.F. Guzowski, C. Bjornsson, W. Shain, and B. Roysam. "A multi-model approach to simultaneous segmentation and classification of heterogeneous populations of cell nuclei in 3D confocal microscope images," *Cytometry A* 2007;71(9):724-36.

[4] R.A. Tyson, D.B.A. Epstein, K.I. Anderson, and T. Bretschneider. "High resolution tracking of cell membrane dynamics in moving cells: An electrifying approach," *Math. Model. Nat. Phenom.* 5(1):34-55, 2010.

[5] S.-C. Chen, T. Zhao, G.J. Gordon, and R.F. Murphy. A novel graphical model approach to segmenting cell images. *Proc IEEE Symp Comput Intell Bioinform Comput Biol* 2006:1-8.

[6] G. Srinivasa, M.C. Fickus, Y. Guo, A.D. Linstedt, and J. Kovacevic. "Active mask segmentation of fluorescence microscope images," *IEEE Trans Image Proc* 2009;18:1817-1829.

[7] C.-J. Du, M. Marcello, D.G. Spiller, M.R.H. White, and T. Bretschneider. "Interactive segmentation of clustered cells via geodesic commute distance and constrained density weighted Nyström method," *Cytometry A*, 77(12):1137-1147, 2010.

[8] S. Andrews, G. Hamarneh, and A. Saad. "Fast random walker with priors using precomputation for interactive medical image segmentation," *Proc. of MICCAI* 2010.

[9] L. Grady. "Multilabel random walker image segmentation using prior models," *IEEE Conf. CVPR,* 1:763–770, June 2005.

[10] M.J. Black, G. Sapiro, D. Marimont, and D. Heeger. "Robust anisotropic diffusion," *IEEE Trans on Image Proc*, 7(3), 421-432, 1998.

[11] Y. Zhang, B.J. Matuszewski, L.-K. Shark, and C.J. Moore. “Medical image segmentation using new hybrid level-set method,” *IEEE ICBV, MEDi08VIS*, London, 9-11 July, 2008.

[12] L. Grady and A.K. Sinop. "Fast approximate random walker segmentation using eigenvector precomputation," *In IEEE Conf. CVPR*, 1–8, 2008.

[13] D. Martin, C. Fowlkes, D. Tal, and J. Malik. "A database of human segmented natural images and its application to evaluating segmentation algorithms and measuring ecological statistics," ICCV, 416-423, 2001.